Huhtinen, Kukka-Emilia; Törmä, Päivi

Conductivity in flat bands from the Kubo-Greenwood formula

Published in:
Physical Review B

DOI:
10.1103/PhysRevB.108.155108

Published: 05/10/2023

Document Version
Publisher's PDF, also known as Version of record

Please cite the original version:
Huhtinen, K.-E., & Törmä, P. (2023). Conductivity in flat bands from the Kubo-Greenwood formula. *Physical Review B*, *108*(15), Article 155108. https://doi.org/10.1103/PhysRevB.108.155108

Conductivity in flat bands from the Kubo-Greenwood formula

Kukka-Emilia Huhtinen[*] and Päivi Törmä[†]
Department of Applied Physics, Aalto University School of Science, FI-00076 Aalto, Finland

(Received 22 March 2023; revised 29 July 2023; accepted 5 September 2023; published 5 October 2023)

Conductivity in a multiband system can be divided into intra- and interband contributions, and the latter further into symmetric and antisymmetric parts. In a flat band, intraband conductivity vanishes and the antisymmetric interband contribution, proportional to the Berry curvature, corresponds to the anomalous Hall effect. We investigate whether the symmetric interband conductivity, related to the quantum metric, can be finite in the zero frequency and flat band limit. Starting from the Kubo-Greenwood formula with a finite scattering rate η, we show that the DC conductivity is zero in a flat band when taking the clean limit ($\eta \to 0$). If commonly used approximations involving derivatives of the Fermi distribution are used, finite conductivity appears at zero temperature $T = 0$; we show however that this is an artifact due to the lack of Fermi surfaces in a (partially) flat band. We then analyze the DC conductivity using the Kubo-Streda formula, and note similar problems at $T = 0$. The predictions of the Kubo-Greenwood formula (without the approximation) and the Kubo-Streda formula differ significantly at low temperatures. We illustrate the results within the Su-Schrieffer-Heger model where one expects vanishing DC conductivity in the dimerized limit as the unit cells are disconnected. We discuss the implications of our results to previous work which has proposed the possibility of finite flat band DC conductivity proportional to the quantum metric. Our results also highlight that care should be taken when applying established transport and linear response approaches in the flat band context, since many of them utilize the existence of a Fermi surface and assume scattering to be weak compared to kinetic energy.

DOI: 10.1103/PhysRevB.108.155108

I. INTRODUCTION

Quantum geometry is key to understanding multiband systems. For instance, quantum geometry has been related to superconductivity in flat bands [1–13], orbital magnetic susceptibility [14,15], light-matter interactions [16,17], the intrinsic anomalous and spin Hall effects [18–24], the capacitance [25], and other physical phenomena [26–32]. Quantum geometric quantities determine the phase and amplitude distances between quantum states, and are represented by the quantum geometric tensor [33] whose imaginary (antisymmetric) part is the Berry curvature and real (symmetric) part the quantum metric (Fubini-Study metric). The quantum metric and Berry curvature are particularly central in the properties of flat band systems. Flat bands are interesting platforms for strongly correlated quantum phenomena, and have attracted increased interest due to their relevance in moiré materials [34–44].

Noninteracting particles on flat bands [45,46] are localized and have a diverging effective mass. However, recent results have predicted a nonzero direct current (DC) conductivity weakly sensitive to the inelastic scattering rate [47,48], also found in disorder-induced quasilocalized zero-energy modes in graphene [49]. This result is sensitive to the used approach, and for instance wave-packet propagation methods predict a vanishing conductivity of the zero-energy modes [50,51]. A nonzero or even diverging DC conductivity has also been predicted in disordered nonisolated flat bands [52,53]. In perfectly flat bands, the zero-temperature DC conductivity has been derived to be proportional to the quantum metric [54–56].

The conductivity is often computed using the Kubo-Greenwood formula, which is the noninteracting version of the exact Kubo formula. The Kubo-Greenwood formula can be sensitive to the order in which the relevant limits (zero temperature, zero scattering, zero frequency) are taken [57] or to approximations made for instance in the delta functions [58]. Here, we show that when applied to flat bands, the Kubo-Streda formula can give drastically different results than the Kubo-Greenwood formula obtained directly via an independent particle approximation of the Kubo formula. In particular, if the zero temperature limit is taken before taking the scattering rate to zero, the Kubo-Streda formula can yield a conductivity proportional to the quantum metric in the clean limit. This nonzero DC conductivity does not appear when applying the Kubo-Greenwood formula, which predicts vanishing DC conductivity.

In Sec. II, we first derive the conductivity within the Kubo-Greenwood formula dividing it into intra- and interband contributions and their symmetric and antisymmetric parts. We show how in a flat band, where the intraband conductivity is zero and the antisymmetric interband contributions give the anomalous Hall effect, the symmetric intraband contribution vanishes at small temperatures in the clean limit. This means no DC conductivity. In Sec. III, we then compute the

[*]Present address: Institute for Theoretical Physics, ETH Zürich, CH-8093 Zürich, Switzerland; kukka-emilia.huhtinen@aalto.fi
[†]paivi.torma@aalto.fi

conductivity using the Kubo-Streda formula, and show, using also the sawtooth ladder, the dimerized Su-Schrieffer-Heeger (SSH) model, and the Lieb lattice as examples, that the results differ dramatically from the Kubo-Greenwood formula at low temperatures. We explain the origin of the discrepancy. In Sec. IV, we summarize and discuss our results.

II. KUBO-GREENWOOD FORMULA

The conductivity tensor $\sigma_{ij}(\omega) \equiv \sigma_{ij}(\omega, \boldsymbol{q} = \boldsymbol{0})$ in a noninteracting multiband system is given by the Kubo-Greenwood formula [59]

$$\sigma_{\mu\nu}(\omega) = \frac{e^2}{i\hbar V} \sum_{\boldsymbol{k}} \sum_{mn} \frac{n_F(\epsilon_n(\boldsymbol{k})) - n_F(\epsilon_m(\boldsymbol{k}))}{\epsilon_n(\boldsymbol{k}) - \epsilon_m(\boldsymbol{k})} \times \frac{[j_\mu(\boldsymbol{k})]_{nm}[j_\nu(\boldsymbol{k})]_{mn}}{\epsilon_n(\boldsymbol{k}) - \epsilon_m(\boldsymbol{k}) + \hbar\omega + i\eta}, \tag{1}$$

which is obtained from the Kubo formula [60] by performing an independent electron approximation. The band dispersion of the nth band is given by $\epsilon_n(\boldsymbol{k})$, and the summation over $\boldsymbol{k}$ runs over the first Brillouin zone. The prefactor involving the Fermi-Dirac distribution $n_F(\epsilon) = 1/(e^{\beta\epsilon} + 1)$, with $\beta = 1/(k_B T)$, should be understood as $\partial_\epsilon n_F(\epsilon)|_{\epsilon=\epsilon_n}$ when $\epsilon_n(\boldsymbol{k}) = \epsilon_m(\boldsymbol{k})$ [58]. The infinitesimal imaginary shift η added to the frequency acts as a small inelastic scattering rate or relaxation rate.

The current operators j_μ are obtained from the momentum derivatives of $H_{\boldsymbol{k}}$, defined as $H = \sum_{\boldsymbol{k}} \sum_{\boldsymbol{k}} c^\dagger_{\boldsymbol{k}\alpha}[H_{\boldsymbol{k}}]_{\alpha\beta} c_{\boldsymbol{k}\beta}$ where $c^\dagger_{\boldsymbol{k}\alpha}$ creates a particle with momentum $\boldsymbol{k}$ at orbital α. In terms of the band dispersions $\epsilon_n(\boldsymbol{k})$ and the corresponding Bloch functions $|n_{\boldsymbol{k}}\rangle$, they are given by

$$[j_\mu(\boldsymbol{k})]_{mn} = \partial_{k_\mu}\epsilon_m(\boldsymbol{k})\delta_{mn} + (\epsilon_m(\boldsymbol{k}) - \epsilon_n(\boldsymbol{k}))\langle\partial_{k_\mu} m_{\boldsymbol{k}}|n_{\boldsymbol{k}}\rangle. \tag{2}$$

Another widely used form of the Kubo-Greenwood formula for the diagonal components of $\sigma_{\mu\nu}$ is

$$\sigma_{\mu\mu} = -\frac{e^2}{\hbar\pi V} \sum_{\boldsymbol{k}} \sum_{mn} \int_{-\infty}^{\infty} d\epsilon \, \frac{\partial n_F(\epsilon)}{\partial\epsilon} \times \mathrm{Tr}[\mathrm{Im}[G_{\boldsymbol{k}}(\epsilon + i\eta)] j_\mu(\boldsymbol{k}) \mathrm{Im}[G_{\boldsymbol{k}}(\epsilon + i\eta)] j_\mu(\boldsymbol{k})], \tag{3}$$

where $G_{\boldsymbol{k}}(E) = (E - H_{\boldsymbol{k}})^{-1}$ is the Green's function. The imaginary shift η in this case can be seen as a constant homogenous purely imaginary self-energy, which could for instance describe disorder causing inelastic scattering in the system. Equation (3) is simply the diagonal components of the more general Bastin [61] and Streda [62] formulas. In this paper, we show that when applied to flat bands, Eqs. (3) and (1) give drastically different results at $T = 0$. In order to avoid confusion between the two forms, we will refer to Eq. (1) as the Kubo-Greenwood formula, and to Eq. (3) as the Kubo-Streda formula.

Let us first derive $\mathrm{Re}[\sigma_{\mu\nu}]$ from Eq. (1). The real part of the conductivity can be decomposed in several ways, for instance into so-called Fermi surface and Fermi sea contributions [62–64]. In our case, we choose to split $\sigma_{\mu\nu}$ into intraband, symmetric interband, and antisymmetric interband contributions, similarly to the decomposition used in Ref. [65]. The advantage of this split when considering flat bands is evident: the intraband contribution from a perfectly flat band vanishes exactly, and only the interband part remains. The antisymmetric part of the latter is related to the intrinsic anomalous Hall effect.

In the thermodynamic limit, the intraband contribution to the real part of the conductivity $\sigma^{\mathrm{intra}}_{\mu\nu}$ obtained from Eq. (1) is

$$\mathrm{Re}\,\sigma^{\mathrm{intra}}_{\mu\nu}(\omega) = -\frac{e^2}{\hbar} \sum_n \int_{\mathrm{BZ}} \frac{d^D\boldsymbol{k}}{(2\pi)^D} \left.\frac{\partial n_F(E)}{\partial E}\right|_{E=\epsilon_n(\boldsymbol{k})} \times [j_\mu(\boldsymbol{k})]_{nn}[j_\nu(\boldsymbol{k})]_{nn} \frac{\eta}{(\hbar\omega)^2 + \eta^2} \tag{4}$$

$$= -\frac{e^2}{\hbar} \sum_n \int_{\mathrm{BZ}} \frac{d^D\boldsymbol{k}}{(2\pi)^D} \left.\frac{\partial n_F(E)}{\partial E}\right|_{E=\epsilon_n(\boldsymbol{k})} \times \partial_{k_\mu}\epsilon_n(\boldsymbol{k})\partial_{k_\nu}\epsilon_n(\boldsymbol{k}) \frac{\eta}{(\hbar\omega)^2 + \eta^2}. \tag{5}$$

We have replaced the momentum summation by an integral over the first Brillouin zone, $(1/V)\sum_{\boldsymbol{k}} \to (1/2\pi)^D \int_{\mathrm{BZ}} d^D\boldsymbol{k}$, where D is the dimension of the system. This contribution to the conductivity is the only component present in a single-band model, and gives the same result as the semiclassical Boltzmann theory of transport when taking $\tau = 1/\eta$ as a momentum-independent relaxation time. The intraband contribution is clearly zero in a perfectly dispersionless band.

The total interband contribution is

$$\sigma^{\mathrm{inter}}_{\mu\nu} = -i\frac{e^2}{\hbar} \sum_{m\neq n} \int_{\mathrm{BZ}} \frac{d^D\boldsymbol{k}}{(2\pi)^D} \frac{n_F(\epsilon_n(\boldsymbol{k}))}{\epsilon_n(\boldsymbol{k}) - \epsilon_m(\boldsymbol{k})} \times \left(\frac{[j_\mu(\boldsymbol{k})]_{nm}[j_\nu(\boldsymbol{k})]_{mn}}{\epsilon_n(\boldsymbol{k}) - \epsilon_m(\boldsymbol{k}) + \hbar\omega + i\eta} + \frac{[j_\nu(\boldsymbol{k})]_{nm}[j_\mu(\boldsymbol{k})]_{mn}}{\epsilon_m(\boldsymbol{k}) - \epsilon_n(\boldsymbol{k}) + \hbar\omega + i\eta} \right). \tag{6}$$

Using Eq. (2), we can express the symmetric and antisymmetric parts of the real part of $\sigma^{\mathrm{inter}}_{\mu\nu}$ as

$$\sigma^s_{\mu\nu}(\omega) = -\frac{e^2}{\hbar} \sum_{n\neq m} \int_{\mathrm{B.Z}} \frac{d^D\boldsymbol{k}}{(2\pi)^D} n_F(\epsilon_n(\boldsymbol{k})) \times \mathrm{Re}[\langle\partial_{k_\mu} n_{\boldsymbol{k}}|m_{\boldsymbol{k}}\rangle\langle m_{\boldsymbol{k}}|\partial_{k_\nu} n_{\boldsymbol{k}}\rangle] \times \left(\frac{\eta(\epsilon_n(\boldsymbol{k}) - \epsilon_m(\boldsymbol{k}))}{(\epsilon_n(\boldsymbol{k}) - \epsilon_m(\boldsymbol{k}) + \hbar\omega)^2 + \eta^2} + \frac{\eta(\epsilon_n(\boldsymbol{k}) - \epsilon_m(\boldsymbol{k}))}{(\epsilon_n(\boldsymbol{k}) - \epsilon_m(\boldsymbol{k}) - \hbar\omega)^2 + \eta^2} \right), \tag{7}$$

$$\sigma^a_{\mu\nu}(\omega) = \frac{e^2}{\hbar} \sum_{n\neq m} \int_{\mathrm{BZ}} \frac{d^D\boldsymbol{k}}{(2\pi)^D} n_F(\epsilon_n(\boldsymbol{k})) \times \mathrm{Im}[\langle\partial_{k_\mu} n_{\boldsymbol{k}}|m_{\boldsymbol{k}}\rangle\langle m_{\boldsymbol{k}}|\partial_{k_\nu} n_{\boldsymbol{k}}\rangle] \times \left(\frac{(\epsilon_n(\boldsymbol{k}) - \epsilon_m(\boldsymbol{k}))(\epsilon_n(\boldsymbol{k}) - \epsilon_m(\boldsymbol{k}) + \hbar\omega)}{(\epsilon_n(\boldsymbol{k}) - \epsilon_m(\boldsymbol{k}) + \hbar\omega)^2 + \eta^2} + \frac{(\epsilon_n(\boldsymbol{k}) - \epsilon_m(\boldsymbol{k}))(\epsilon_n(\boldsymbol{k}) - \epsilon_m(\boldsymbol{k}) - \hbar\omega)}{(\epsilon_n(\boldsymbol{k}) - \epsilon_m(\boldsymbol{k}) - \hbar\omega)^2 + \eta^2} \right). \tag{8}$$

The interband contribution is thus related to components of the quantum geometric tensor [66], which for the nth band is

defined as

$$\mathcal{G}^n_{\mu\nu}(\boldsymbol{k}) = 2\langle\partial_{k_\mu} n_{\boldsymbol{k}}|(1 - |n_{\boldsymbol{k}}\rangle\langle n_{\boldsymbol{k}}|)|\partial_{k_\nu} n_{\boldsymbol{k}}\rangle \tag{9}$$

$$= 2\sum_{m:m\neq n}\langle\partial_{k_\mu} n_{\boldsymbol{k}}|m_{\boldsymbol{k}}\rangle\langle m_{\boldsymbol{k}}|\partial_{k_\nu} n_{\boldsymbol{k}}\rangle. \tag{10}$$

The real and imaginary parts of $\mathcal{G}^n_{\mu\nu} = \mathcal{M}^n_{\mu\nu} + i\mathcal{B}^n_{\mu\nu}$ are the quantum metric and Berry curvature, respectively. Since the quantum geometric tensor is Hermitian, the quantum metric is symmetric while the Berry curvature is antisymmetric.

In the limit $\omega \to 0$, $\eta \to 0^+$, we recover for $\sigma^a_{\mu\nu}$ the well-known relationship between the intrinsic anomalous Hall conductivity and the Berry curvature [18–22,67]:

$$\sigma^a_{\mu\nu}(\omega = 0) = \frac{e^2}{\hbar}\sum_n \int_{\mathrm{BZ}} \frac{d^D\boldsymbol{k}}{(2\pi)^D} n_F(\epsilon_n(\boldsymbol{k}))\mathcal{B}^n_{\mu\nu}(\boldsymbol{k}). \tag{11}$$

Notably, the antisymmetric part of the conductivity can be nonzero even on a flat band in the clean limit $\eta \to 0^+$. In contrast to for instance the superfluid weight and Drude weight, it also generally depends on the choice of orbital positions within a unit cell [10,68].

The symmetric interband contribution, on the other hand, is related to band-resolved components of the quantum metric, but these components are weighted by factors depending on the band dispersions. In the limit $\eta \to 0^+$, $\eta/(x^2 + \eta^2) \to \pi\delta(x)$, and the symmetric interband conductivity becomes

$$\begin{aligned}\sigma^s_{\mu\nu}(\omega) = -\frac{e^2\pi}{\hbar}\sum_{n\neq m}\int_{\mathrm{BZ}} \frac{d^D\boldsymbol{k}}{(2\pi)^D} n_F(\epsilon_n(\boldsymbol{k}))\\ \times \mathrm{Re}[\langle\partial_{k_\mu} n_{\boldsymbol{k}}|m_{\boldsymbol{k}}\rangle\langle m_{\boldsymbol{k}}|\partial_{k_\nu} n_{\boldsymbol{k}}\rangle](\epsilon_n(\boldsymbol{k}) - \epsilon_m(\boldsymbol{k}))\\ \times (\delta(\epsilon_n(\boldsymbol{k}) - \epsilon_m(\boldsymbol{k}) + \hbar\omega)\\ + \delta(\epsilon_n(\boldsymbol{k}) - \epsilon_m(\boldsymbol{k}) - \hbar\omega)).\end{aligned} \tag{12}$$

When all bands are isolated from each other, $|\epsilon_n - \epsilon_m| \geqslant E_{\mathrm{gap,min}}$ for $m \neq n$, where $E_{\mathrm{gap,min}}$ is the smallest interband gap. One can see from the delta functions in Eq. (12) that the interband conductivity then vanishes for any frequency $|\hbar\omega| < E_{\mathrm{gap,min}}$ in the clean limit. It follows that the symmetric part of the DC conductivity in an isolated flat band is zero in the limit $\eta \to 0^+$. At nonzero scattering rate, the DC conductivity can acquire a nonzero value because of the spread of the Lorentzian functions centered at frequencies $|\hbar\omega| \geqslant E_{\mathrm{gap,min}}$; this is just the finite linewidth of interband transitions resonant with an AC field. For $\eta \ll E_{\mathrm{gap,min}}$, this nonzero interband contribution is approximately

$$\begin{aligned}\sigma^s_{\mu\nu}(\omega = 0) \approx -2\eta\frac{e^2}{\hbar}\sum_n \int_{\mathrm{BZ}} \frac{d^D\boldsymbol{k}}{(2\pi)^D} n_F(\epsilon_n(\boldsymbol{k}))\\ \times \sum_{m:m\neq n} \frac{\mathrm{Re}[\langle\partial_{k_\mu} n_{\boldsymbol{k}}|m_{\boldsymbol{k}}\rangle\langle m_{\boldsymbol{k}}|\partial_{k_\nu} n_{\boldsymbol{k}}\rangle]}{\epsilon_n(\boldsymbol{k}) - \epsilon_m(\boldsymbol{k})},\end{aligned} \tag{13}$$

where we have approximated $\eta(\epsilon_n(\boldsymbol{k}) - \epsilon_m(\boldsymbol{k}))/[(\epsilon_n(\boldsymbol{k} - \epsilon_m(\boldsymbol{k})))^2 + \eta^2] \approx \eta/(\epsilon_n(\boldsymbol{k}) - \epsilon_m(\boldsymbol{k}))$. The linear dependence on the scattering rate is consistent with the result obtained in Refs. [54,65] for small scattering rates in a dispersive bands and in Ref. [69] in flat bands at a nonzero temperature. Here, this holds also for perfectly flat bands at $T = 0$. The interband conductivity given by Eq. (13) does not generally involve the quantum metric of band n directly because of the division by $\epsilon_n(\boldsymbol{k}) - \epsilon_m(\boldsymbol{k})$ in the sum. An exception would be for instance a two-band model with only flat bands, where this difference would be a momentum-independent constant, and the sum over m would indeed yield the quantum metric of band n at momentum $\boldsymbol{k}$.

We note that an expression which relates the DC conductivity directly to the quantum metric can be obtained from Eq. (12) by using that

$$\begin{aligned}\frac{n_F(\epsilon_n) - n_F(\epsilon_m)}{\epsilon_n - \epsilon_m}\delta(\epsilon_n - \epsilon_m + \hbar\omega)\\ = \frac{n_F(\epsilon_n + \hbar\omega) - n_F(\epsilon_n)}{\hbar\omega}\delta(\epsilon_n - \epsilon_m + \hbar\omega).\end{aligned} \tag{14}$$

The prefactor on the second line should be, as mentioned earlier, understood as the derivative $\partial n_F(E)/\partial E|_{E=\epsilon_n(\boldsymbol{k})}$ when $\omega \to 0$. If the delta functions are replaced by Lorentzian functions after this substitution, the DC conductivity for $\eta \ll E_{\mathrm{gap,min}}$ becomes

$$\begin{aligned}\sigma^s_{\mu\nu}(\omega = 0) = -\eta\frac{e^2}{\hbar}\sum_n \int_{\mathrm{BZ}} \frac{d^D\boldsymbol{k}}{(2\pi)^D} \left.\frac{\partial n_F(E)}{\partial E}\right|_{E=\epsilon_n(\boldsymbol{k})}\\ \times \sum_{m\neq n}\mathrm{Re}[\langle\partial_{k_\mu} n_{\boldsymbol{k}}|m_{\boldsymbol{k}}\rangle\langle m_{\boldsymbol{k}}|\partial_{k_\nu} n_{\boldsymbol{k}}\rangle].\end{aligned} \tag{15}$$

This form is more reminiscent of results obtained for instance by computing the conductivity in Matsubara space [54,65]. It should however be stressed that here this is an approximation, as Eq. (14) no longer holds if the delta function is replaced by a Lorentzian function with a finite spread. In the limit $\omega \to 0$, the prefactor on the right-hand side of Eq. (14) is replaced by a derivative of the Fermi-Dirac distribution at ϵ_n, which approximates $[n_F(\epsilon_n) - n_F(\epsilon_m)]/(\epsilon_n - \epsilon_m)$ on the left hand side only when ϵ_n and ϵ_m are close. If the bands are well isolated, this does not hold. Equation (15) is also problematic at $T = 0$ if the Fermi energy is in a perfectly flat band, as the derivative of the Fermi-Dirac distribution would then become $-\delta(E_{\mathrm{FB}} - \mu) = -\delta(0)$, where E_{FB} is the energy of the flat band, at all points of the Brillouin zone. Transforming the integral over the momentum to an integral over the energy does not help, as it would involve the density of states on the flat band, which diverges. However, at any nonzero temperature, Eqs. (15) and (13) always give the same vanishing interband DC conductivity in the $\eta \to 0^+$ limit.

A vanishing DC conductivity on a noninteracting isolated flat band is unsurprising, since single particles are localized. However, it contrasts with recent results at $T = 0$, which have found a nonzero DC conductivity proportional to the quantum metric even in the limit $\eta \to 0^+$ [48,54–56]. In Refs. [54,65], it was shown that the interband contribution vanishes linearly with η on dispersive bands even at $T = 0$, and this finite conductivity in the clean limit thus appears only in perfectly flat bands. In the following, we show that such results can arise when applying the Kubo-Streda formula when the Fermi energy is in a (partially) flat band. This is related to contributions from states at exactly the Fermi energy which do not vanish in the clean limit, present in the Streda formula but absent in the Kubo-Greenwood formula [Eq. (1)]. These contributions only

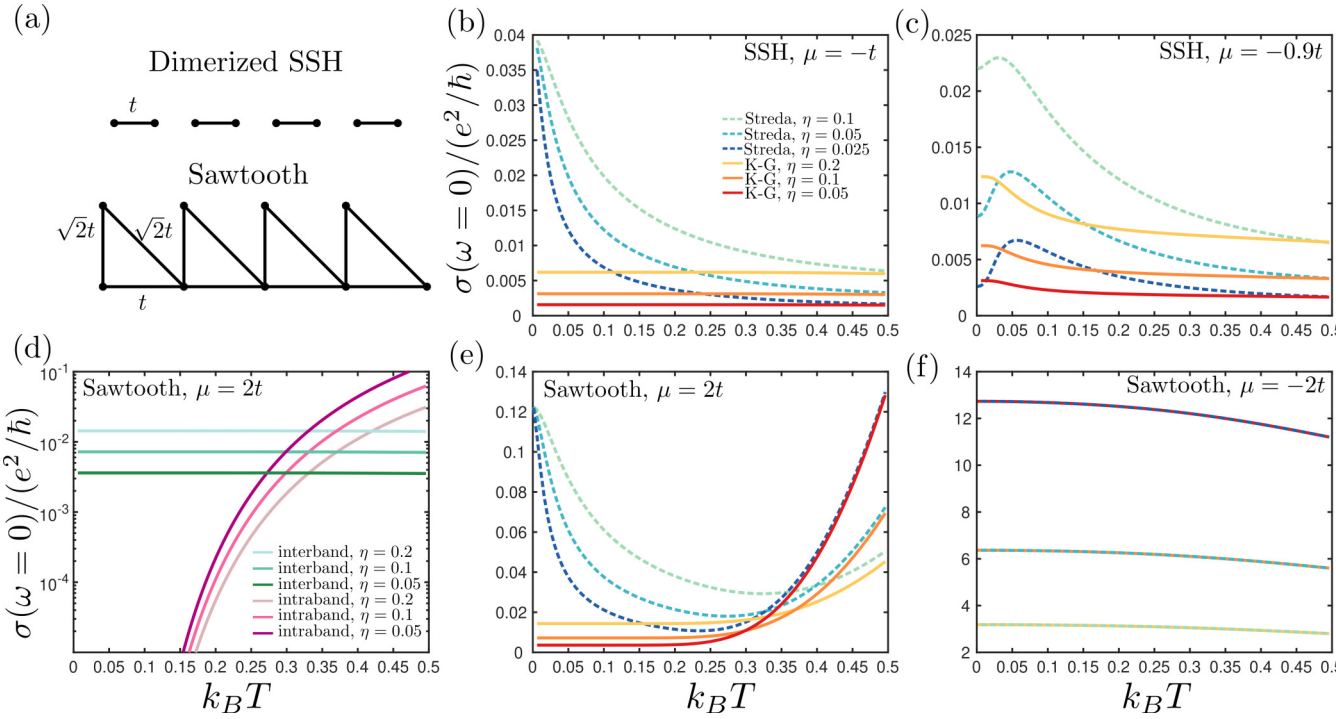

FIG. 1. (a) Sketch of the dimerized SSH model and the sawtooth ladder studied here. (b, c) DC conductivity in the SSH model at $\mu = -t$, when the chemical potential is in the lowest flat band (b), and at $\mu = -0.9t$ (c). The conductivity obtained from the Kubo-Greenwood formula consists of solely interband contributions, and vanishes at all temperatures in the clean limit $\eta \to 0^+$. The DC conductivity obtained from the Kubo-Streda formula remains pinned at $1/(8\pi)$ at $T = 0$, but vanishes for nonzero temperatures. When the chemical potential is tuned away from the flat band, the limit $\eta \to 0^+$ from the Kubo-Greenwood and Kubo-Streda formulas is the same, although the behavior at nonzero η is drastically different. (d) Interband and intraband contributions obtained from the Kubo-Greenwood formula in the sawtooth ladder when the chemical potential is in the flat band. The intraband contribution from the dispersive band diverges as $\eta \to 0^+$, whereas the interband contribution vanishes. (e, f) DC conductivity from the Kubo-Greenwood and Kubo-Streda formula when the chemical potential is (e) in the flat band and (f) in the middle of the dispersive band. In a dispersive band, both methods give the same results, whereas in a flat band, they give drastically different results. In the flat band, the conductivity from the Kubo-Streda formula remains pinned to $2/(3\sqrt{3}\pi)$ at $T = 0$.

become meaningful in systems without a Fermi surface, such as a flat band.

III. FLAT BAND CONDUCTIVITY FROM THE KUBO-STREDA FORMULA

The Kubo-Streda formula gives the symmetric part of the DC conductivity as [62–64]

$$\sigma^{\mathrm{sym}}_{\mu\nu}(\omega = 0) = -\frac{e^2}{\hbar\pi}\int_{-\infty}^{\infty} \mathrm{d}\epsilon \frac{\partial n_F(\epsilon)}{\partial \epsilon} \times \mathrm{Tr}[\mathrm{Im}[G_{\boldsymbol{k}}(\epsilon + i\eta)] j_\mu(\boldsymbol{k}) \times \mathrm{Im}[G_{\boldsymbol{k}}(\epsilon + i\eta)] j_\nu(\boldsymbol{k})]. \quad (16)$$

This equation can be derived from the Kubo-Greenwood formula directly, or can be obtained from the exact Kubo formula by computing the current-current response function in Matsubara space assuming noninteracting particles. When applied to dispersive bands, Eqs. (1) and (16) usually give very close results, provided we take $\eta_{\mathrm{KG}} = 2\eta_{\mathrm{Streda}}$. However, when applied to flat bands, the DC conductivities can differ drastically especially at low temperatures.

To illustrate this, we consider two one-dimensional flat band systems: the sawtooth ladder and the dimerized limit of the SSH model [see Fig. 1(a)]. We describe these systems with the tight-binding Hamiltonian $H = \sum_{i\alpha,j\beta} t_{i\alpha,j\beta} c^\dagger_{i\alpha} c_{j\beta} - \mu \sum_{i\alpha} n_{i\alpha}$, where $t_{i\alpha,j\beta}$ is the hopping amplitude from site $j\beta$ to $i\alpha$. The unit cells are labeled with i and j, while α and β indicate the orbitals within a unit cell. By taking the Fourier transformation $c_{i\alpha} = (1/\sqrt{N_c}) \sum_{\boldsymbol{k}} c_{\boldsymbol{k}\alpha} e^{i\boldsymbol{k}\cdot(\boldsymbol{R}_i + \boldsymbol{\delta}_\alpha)}$ the Hamiltonian becomes $H = \sum_{\boldsymbol{k}} c^\dagger_{\boldsymbol{k}\alpha} [H_{\boldsymbol{k}}]_{\alpha\beta} c_{\boldsymbol{k}\alpha}$, where

$$H_{\boldsymbol{k}} = \sum_i \sum_{\alpha\beta} t_{i\alpha,0\beta} e^{-i\boldsymbol{k}\cdot(\boldsymbol{R}_i + \boldsymbol{\delta}_\alpha - \boldsymbol{\delta}_\beta)}. \quad (17)$$

Here, $\boldsymbol{R}_i$ is the position of the ith unit cell, and $\boldsymbol{\delta}_\alpha = \boldsymbol{r}_{i\alpha} - \boldsymbol{R}_i$, with $\boldsymbol{r}_{i\alpha}$ the position of site $i\alpha$. The eigenvalues and eigenvectors give the band dispersion relations $\epsilon_n(\boldsymbol{k})$ and the periodic parts of the Bloch functions $|n_{\boldsymbol{k}}\rangle$, respectively.

Note that in a multiband lattice taking the orbital positions $\boldsymbol{\delta}_\alpha$ into account in the Fourier transformation is essential in order to obtain the correct conductivity [65,70,71]. This is in contrast to the superfluid weight, which is independent of the particular choice of $\boldsymbol{\delta}_\alpha$ provided it is computed accurately [10]. In other words, the conductivity is generally geometry dependent, using the terminology introduced in Ref. [68].

The sawtooth ladder features a perfectly flat band at energy $E = 2t$, isolated from a dispersive band $\epsilon(\boldsymbol{k}) = -[2 + 2\cos(k)]t$. The dimerized SSH model has two exactly flat bands at energies $E = \pm t$. Importantly, the dimerized SSH

model consists of two-site clusters that are completely disconnected from each other. It is thus reasonable to expect the DC conductivity to vanish.

As can be seen from Fig. 1, when the chemical potential is tuned into the flat band, the interband conductivity obtained from Eq. (1) vanishes in the clean limit $\eta \to 0^+$ in all cases. In the SSH model, the intraband conductivity is exactly zero because the system contains only flat bands, and the Kubo-Greenwood formula predicts a vanishing $\sigma(\omega = 0)$ [Figs. 1(b) and 1(c)]. In the sawtooth ladder [Figs. 1(d) and 1(e)], the intraband contribution from the dispersive band is nonzero at any $T > 0$, and diverges in the limit $\eta \to 0^+$. However, it is highly suppressed at low temperatures even for small η when the chemical potential is in the flat band. At the values of η used here, the interband conductivity is dominant up to a temperature $k_B T \approx 0.3$. This threshold temperature decreases with the scattering rate η and reaches zero in the limit $\eta \to 0$. The nonzero conductivity found at nonzero η thus mostly arises from the interband contribution, related to the quantum geometry of the bands, at low temperatures, which is expected due to the flatness of the band.

The conductivity obtained from Eq. (16), the Kubo-Streda formula, is drastically different from the one obtained using the Kubo-Greenwood formula. At exactly $T = 0$, it retains a nonzero value proportional to the integrated quantum metric even when $\eta \to 0^+$ [Figs. 1(b) and 1(e)]. For $T > 0$, the interband conductivity vanishes for both formulas in the limit $\eta \to 0^+$. As a consequence, the limits $\eta \to 0^+$ and $T \to 0$ do not commute when applying the Kubo-Streda formula. The qualitative behavior obtained from Eqs. (16) and (1) at nonzero η is very different at low temperatures. The interband conductivity obtained from the Kubo-Greenwood formula varies little with temperature when the chemical potential is tuned into the flat band, whereas the Kubo-Streda formula predicts a conductivity roughly proportional to T^{-1}, similar to the one found at nonzero temperatures for topological flat bands in Ref. [69]. A notable difference in behavior subsists when the chemical potential is tuned slightly away from the flat band, as can be seen from Fig. 1(c), although both formulas then give the same conductivity in the limit $\eta \to 0^+$. When no flat band exists in the vicinity of the chemical potential, both Eqs. (16) and (1) predict a similar conductivity provided the scattering rates are related by a factor of 2.

The two models studied above feature only isolated flat bands, for which the Kubo-Greenwood formula predicts a vanishing DC conductivity. However, in the presence of a band touching, the assumption that $\eta \ll E_{\text{gap,min}}$, which is essential to obtain an interband conductivity proportional to η, no longer holds for any $\eta > 0$. We thus compute the conductivity in the Lieb lattice, a two-dimensional bipartite lattice featuring a single flat band which touches dispersive bands at the corners of the Brillouin zone [see Fig. 2(a)].

The intraband and interband components of the conductivity obtained from the Kubo-Greenwood formula for the Lieb lattice are shown in Fig. 2(c). The intraband conductivity in this model is less strongly suppressed than in the sawtooth ladder, which is expected since the flat band is no longer isolated. The interband contribution to the conductivity is however still dominant below a threshold temperature decreasing with η. In contrast to the sawtooth ladder, the interband conductivity does not seem to vanish even in the limit $\eta \to 0^+$ and $T \to 0$, and instead retains a finite value. This is due to the band touching, which corresponds to a divergence of the quantum metric of the flat band at the corners of the Brillouin zone. To verify whether this finite value depends on the choice of positions in the unit cell, we computed the interband conductivity when the intraunit cell positions of all orbitals within a unit cell are the same, i.e., $\boldsymbol{\delta}_\alpha = \mathbf{0}$ for all α. As shown in the inset of Fig. 2(c), the conductivity in the limit $\eta \to 0^+$ does not depend on the choice of basis. However, for finite η, the result does slightly vary based on the positions in a unit cell.

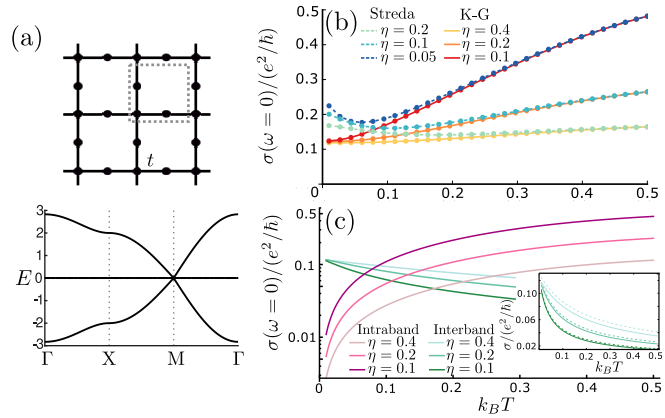

FIG. 2. (a) The Lieb lattice (top) and its band dispersions (bottom). The unit cell is indicated by a dashed box. (b) Conductivity obtained from the Kubo-Streda formula (dashed lines) and the Kubo-Greenwood formula (full lines) as a function of temperature. The two results agree very well at high temperatures when the scattering rates are related by a factor of 2, but become increasingly different as the temperature is decreased. (c) Interband and intraband contributions to the conductivity obtained from the Kubo-Greenwood formula. Note the logarithmic conductivity axis. Inset: Interband conductivity obtained for the symmetric positions shown in (a) (full lines), and when $\boldsymbol{\delta}_\alpha = \mathbf{0}$, meaning all orbitals within a unit cell are at the same spatial position (dashed lines).

Again in this case, the results obtained from the Kubo-Streda formula, shown in Fig. 2(b), differ significantly from those of the Kubo-Greenwood formula at low temperatures. Whereas the conductivity predicted by the Kubo-Greenwood formula acquires a finite value in the limit $T \to 0$, the conductivity given by the Kubo-Streda formula diverges. This reflects the fact that the integrated quantum metric of the flat band also diverges due to the band touching point.

These results point to a discrepancy between the results given by the Kubo-Greenwood and Kubo-Streda formulas when computing the conductivity in flat bands. This discrepancy is the most remarkable near zero temperature, where the interband contribution involving the flat band is the most prominent. For an isolated flat band, the Kubo-Greenwood formula predicts a vanishing DC conductivity at $T = 0$ in the clean limit, whereas the Kubo-Streda formula gives a conductivity proportional to the quantum metric.

Origin of the discrepancy

In order to understand the differences in the results obtained from Eqs. (16) and (1), let us derive Eq. (16) from Eq. (1).

Starting from Eq. (1), we write

$$\sigma_{\mu\nu}(\omega=0) = -i\frac{e^2}{\hbar}\int_{\mathrm{BZ}}\frac{d^D\boldsymbol{k}}{(2\pi)^D}\int_{-\infty}^{\infty}d\epsilon\sum_{mn}[j_\mu]_{nm}[j_\nu]_{mn} \times\left(\frac{n_F(\epsilon)\delta(\epsilon-\epsilon_n)}{(\epsilon-\epsilon_m)(\epsilon-\epsilon_m+i\eta)} - \frac{n_F(\epsilon)\delta(\epsilon-\epsilon_m)}{(\epsilon_n-\epsilon)(\epsilon_n-\epsilon+i\eta)}\right). \tag{18}$$

Using that $\lim_{\eta\to0^+}1/[(\epsilon-\epsilon_n)(\epsilon-\epsilon_n+i\eta)] = -\lim_{\eta\to0^+}\partial_\epsilon(\epsilon-\epsilon_n+i\eta)^{-1}$, we obtain the Kubo-Bastin formula

$$\sigma_{\mu\nu}(\omega=0) = i\frac{e^2}{\hbar}\int_{\mathrm{BZ}}\frac{d^D\boldsymbol{k}}{(2\pi)^D}\int_{-\infty}^{\infty}d\epsilon\, n_F(\epsilon) \times\mathrm{Tr}\left[j_\mu\frac{\partial G_{\boldsymbol{k}}(\epsilon+i\eta)}{\partial\epsilon}j_\nu\delta(\epsilon-H) - j_\mu\delta(\epsilon-H)j_\nu\frac{\partial G_{\boldsymbol{k}}(\epsilon-i\eta)}{\partial\epsilon}\right]. \tag{19}$$

A detailed derivation of the full Kubo-Streda formula from this form is given by Crépieux and Bruno in Ref. [63]. Here, we will focus on the symmetric part of the conductivity, which reads

$$\sigma^{\mathrm{sym}}_{\mu\nu}(\omega=0) = \frac{e^2}{\hbar}\int_{\mathrm{BZ}}\frac{d^D\boldsymbol{k}}{(2\pi)^D}\int_{-\infty}^{\infty}d\epsilon\, n_F(\epsilon) \times\mathrm{Tr}\left[j_\mu\frac{\partial}{\partial\epsilon}\mathrm{Im}[G(\epsilon-i\eta)]j_\nu\delta(\epsilon-H) + j_\mu\delta(\epsilon-H)j_\nu\frac{\partial}{\partial\epsilon}\mathrm{Im}[G(\epsilon-i\eta)]\right]. \tag{20}$$

If we replace the delta functions by a Lorentzian, we can write $\pi\delta(\epsilon-H) = \lim_{\eta'\to0^+}\mathrm{Im}G(\epsilon-i\eta')$, where η' can generally be different from the scattering rate in $G(\epsilon-i\eta)$. With $\eta'=\eta$, we obtain precisely the formula (16) through integration by parts. Taking $\eta'=\eta$ should not change the result in the clean limit as long as the limit $\lim_{\eta'\to0^+,\eta\to0^+}$ does not depend on the direction it is taken in. However, this is not always the case at $T=0$. At exactly zero temperature, Eq. (20) becomes $\sigma^{\mathrm{sym}}_{\mu\nu}(\omega=0) = \sigma^{\mathrm{I}}_{\mu\nu} + \sigma^{\mathrm{II}}_{\mu\nu}$, where

$$\sigma^{\mathrm{I}}_{\mu\nu} = \frac{e^2}{2\hbar\pi}\int_{\mathrm{BZ}}\frac{d^D\boldsymbol{k}}{(2\pi)^D}\mathrm{Tr}\left[j_\mu\mathrm{Im}[G(\mu-i\eta)]j_\nu\mathrm{Im}[G(\mu-i\eta')] + j_\mu\mathrm{Im}[G(\mu-i\eta')]j_\nu\mathrm{Im}[G(\mu-i\eta)]\right] \tag{21}$$

$$= \frac{e^2}{2\hbar\pi}\sum_{mn}\int_{\mathrm{BZ}}\frac{d^D\boldsymbol{k}}{(2\pi)^D}\left(\frac{\eta\eta'}{[(\epsilon_n-\mu)^2+\eta^2][(\epsilon_m-\mu)^2+\eta'^2]} + \frac{\eta\eta'}{[(\epsilon_n-\mu)^2+\eta'^2][(\epsilon_m-\mu)^2+\eta^2]}\right)[j_\mu]_{mn}[j_\nu]_{nm}, \tag{22}$$

$$\sigma^{\mathrm{II}}_{\mu\nu} = \frac{e^2}{2\hbar\pi}\int_{\mathrm{BZ}}\frac{d^D\boldsymbol{k}}{(2\pi)^D}\int_{-\infty}^{\mu}d\epsilon\,\mathrm{Tr}\left[j_\mu\frac{\partial}{\partial\epsilon}\mathrm{Im}[G(\epsilon-i\eta)]j_\nu\mathrm{Im}[G(\epsilon-i\eta')] + j_\mu\mathrm{Im}[G(\epsilon-i\eta')]j_\nu\frac{\partial}{\partial\epsilon}\mathrm{Im}[G(\epsilon-i\eta)] - j_\mu\mathrm{Im}[G(\epsilon-i\eta)]j_\nu\frac{\partial}{\partial\epsilon}\mathrm{Im}[G(\epsilon-i\eta')] - j_\mu\frac{\partial}{\partial\epsilon}\mathrm{Im}[G(\epsilon-i\eta')]j_\nu\mathrm{Im}[G(\epsilon-i\eta)]\right]. \tag{23}$$

The contribution $\sigma^{\mathrm{I}}_{\mu\nu}$ causes the discrepancy between the Kubo-Greenwood and the Kubo-Streda formula in flat bands. Note that the double limit $\lim_{\eta\to0^+,\eta'\to0^+}$ of $\eta\eta'/[((\epsilon_n-\mu)^2+\eta^2)((\epsilon_m-\mu)^2+\eta'^2)]$ depends on the direction of the limits whenever only one of ϵ_n or ϵ_m is equal to μ. For instance, if $\epsilon_n=\mu$ and $\epsilon_m\neq\mu$, the limit diverges if we first take $\eta\to0^+$, vanishes if we take $\eta'\to0^+$ before $\eta\to0^+$, and gives the nonzero finite result $1/(\epsilon_m-\epsilon_n)^2$ if $\eta=\eta'$. The integrand in Eq. (22) is thus problematic whenever one of ϵ_n or ϵ_m is equal to the Fermi energy. In other words, the contribution coming from states at the Fermi energy to the interband part of the conductivity can be inaccurate.

In a dispersive band where the Fermi surface is $D-1$ dimensional, the states at exactly the Fermi energy will not contribute in the thermodynamic limit, since their area in the Brillouin zone vanishes. However, if the Fermi energy is in a (partially) flat band, these contributions appear in the final result. In particular, if we set $\eta=\eta'$ when taking the clean limit, the resulting DC conductivity when the chemical potential is tuned into a flat band is proportional to the integrated quantum metric of the flat band n:

$$\sigma_{\mu\nu} = \frac{e^2}{\hbar\pi}\int_{\mathrm{BZ}}\frac{d^D\boldsymbol{k}}{(2\pi)^D}\sum_{m\neq n}\langle\partial_\mu n_{\boldsymbol{k}}|m_{\boldsymbol{k}}\rangle\langle m_{\boldsymbol{k}}|\partial_\nu n_{\boldsymbol{k}}\rangle. \tag{24}$$

However, this is only the case when taking the limit along $\eta=\eta'$, and the double limit is actually not well defined.

The source of the problem is the introduction of the derivative of the Fermi distribution. Above, we already mentioned that integrating $\partial n_F(\epsilon)/\partial\epsilon|_{\epsilon=\epsilon_n(\boldsymbol{k})}$ over the Brillouin zone causes problems when $\epsilon_n(\boldsymbol{k})$ is constant. Here, it may appear that the same problem is no longer present, because we could integrate $\partial n_F(\epsilon)/\partial\epsilon|_{\epsilon=\epsilon_n(\boldsymbol{k})}$ over the energy ϵ. However, if we take $\eta'\to0^+$ first before $\eta\to0^+$, we recover the delta function first introduced in Eq. (18). Now that we already integrated over the energy to get rid of the delta function coming from $\partial n_F(\epsilon)/\partial\epsilon|_{\epsilon=\epsilon_n(\boldsymbol{k})}$, the remaining delta function has transformed into $\delta[\mu-\epsilon_n(\boldsymbol{k})]$. Again, the integral over the Brillouin zone is no longer well defined when the chemical potential is in a dispersionless flat band.

We note that these problems are less likely to appear when computing the antisymmetric part of the conductivity, relevant for the anomalous Hall effect, since the equations for its evaluation typically involve the Fermi distribution and not its derivative. Then, no ill-defined integrals of delta functions appear at $T = 0$.

IV. CONCLUSIONS AND DISCUSSION

We calculated the DC conductivity in multiband systems using the Kubo-Greenwood formula and the Kubo-Streda formula, and scrutinized various approximations used in the literature. Our focus was analyzing the DC conductivity in an isolated (gapped from other bands) flat band and its potential connection to quantum geometry. We summarize here our findings and discuss their implications.

The Kubo-Greenwood formalism, without approximate use of derivatives of the Fermi function, predicts vanishing DC conductivity in a flat band in the clean limit $\eta \to 0$. This is physically intuitive considering that single particles have infinite effective mass and DC conductivity is essentially single-particle transport in a system with no correlations but only a (vanishingly small) scattering rate η. The Kubo-Greenwood formula gives a vanishing DC conductivity in the clean limit in the dimerized SSH chain, consistent with the fact that transport through the chain is impossible since it is disconnected. In our view, the Kubo-Greenwood result of zero DC conductivity is the physically correct description of noninteracting electron transport in a flat band.

At finite η, the Kubo-Greenwood formula gives a DC conductivity related to the quantum geometry of the bands, but this is simply the DC tail of the AC conductivity resonance at the band-gap frequency. Whether the conductivity obtained from the Kubo-Greenwood formula at finite η is in any way representative of a realistic system is questionable, as a constant homogenous scattering rate does not generally fully describe effects such as disorder.

The Kubo-Streda formula gives results very different from the Kubo-Greenwood one in a flat band, and we argue they do not describe the limit of a dispersionless band correctly. This becomes apparent when they predict finite DC conductivity at zero temperature even in the completely disconnected SSH model where a DC current through the system clearly cannot flow. Moreover, the nonzero interband DC conductivity in the clean limit arises only for *perfectly* flat bands: as soon as even a small dispersion is added, the conductivity at low η becomes proportional to η on an isolated band. Since a perfectly flat band never occurs in practice in an experimental setting, the nonzero conductivity predicted for isolated perfectly flat bands would not be likely to be observed even if it was accurate. The Kubo-Greenwood formula predicts the same conductivity for both a perfectly flat band and a dispersive band with a vanishingly small width.

We point out in detail where the problems with the Kubo-Streda formula arise: essentially, they boil down to the lack of a Fermi surface. In a flat band, the Fermi energy is massively degenerate and forms a volume (in three dimensions) or a surface (in two dimensions) in momentum space. Therefore any unphysical features at the Fermi energy arising from approximations become finite, while in a dispersive band they would vanish within an integral over the Brillouin zone since there the Fermi surface is an area (in three dimensions) or a line (in two dimensions) of zero measure. One might think this could be solved by changing the integration variable from momentum to energy, but that would involve introducing the density of states which diverges in a flat band, the same problem dressed in a different way. Thus, in general, in studies of linear response phenomena in the flat band limit, one needs to be cautious with commonly applied approximations and formulas, since many of them are valid and physically meaningful only in the presence of a Fermi surface. Several recent studies of conductivity in a flat band [47–49,55,56,69] should probably be revisited to understand the potential implications of our results there.

Our results relate also to the subtle connections between quantum geometry, physical observables, and the orbital positions in a lattice system. The symmetric and antisymmetric components of the quantum geometric tensor, namely the quantum metric and Berry curvature, depend on orbital positions, i.e., change of orbital coordinates while keeping the connectivity (hopping) between the orbitals the same. It is well known that many physical observables, such as the anomalous Hall conductivity, are determined by the Berry curvature and thus depend on orbital positions. Flat band superconductivity was predicted to be proportional to the quantum metric (which is orbital dependent) within a large number of studies (see Refs. [1,44] and references therein), while the definition of the superfluid weight is clearly independent of orbital positions. This discrepancy was solved only recently by showing that the superfluid weight is actually related to the minimal quantum metric, an orbital-independent quantity [10]. Here we showed that the flat band AC conductivity can have a relation to the quantum metric, while the DC conductivity in the limit $\eta \to 0^+$ does not depend on the choice of basis. We believe that it is probably possible to determine, at a general level, which physical observables are orbital-position dependent simply based on Maxwell's equations, general properties of the (superconducting or single electron) wave function, and gauge invariance. We leave this to a future work. Another important future research problem is to analyze transport in the case where other bands are touching the flat band.

ACKNOWLEDGMENTS

We thank Johannes Mitscherling for useful discussions. We acknowledge support by the Academy of Finland under Project No. 349313. K.-E.H. acknowledges financial support by the Magnus Ehrnrooth Foundation.

[1] S. Peotta and P. Törmä, Superfluidity in topologically nontrivial flat bands, Nat. Commun. **6**, 8944 (2015).

[2] L. Liang, T. I. Vanhala, S. Peotta, T. Siro, A. Harju, and P. Törmä, Band geometry, Berry curvature, and superfluid weight, Phys. Rev. B **95**, 024515 (2017).

[3] A. Julku, S. Peotta, T. I. Vanhala, D.-H. Kim, and P. Törmä, Geometric origin of superfluidity in the Lieb-lattice flat band, Phys. Rev. Lett. **117**, 045303 (2016).

[4] E. Rossi, Quantum metric and correlated states in two-dimensional systems, Curr. Opin. Solid State Mater. Sci. **25**, 100952 (2021).

[5] P. Törmä, L. Liang, and S. Peotta, Quantum metric and effective mass of a two-body bound state in a flat band, Phys. Rev. B **98**, 220511(R) (2018).

[6] A. Julku, T. J. Peltonen, L. Liang, T. T. Heikkilä, and P. Törmä, Superfluid weight and Berezinskii-Kosterlitz-Thouless transition temperature of twisted bilayer graphene, Phys. Rev. B **101**, 060505(R) (2020).

[7] X. Hu, T. Hyart, D. I. Pikulin, and E. Rossi, Geometric and conventional contribution to the superfluid weight in twisted bilayer graphene, Phys. Rev. Lett. **123**, 237002 (2019).

[8] F. Xie, Z. Song, B. Lian, and B. A. Bernevig, Topology-bounded superfluid weight in twisted bilayer graphene, Phys. Rev. Lett. **124**, 167002 (2020).

[9] M. Iskin, Two-body problem in a multiband lattice and the role of quantum geometry, Phys. Rev. A **103**, 053311 (2021).

[10] K.-E. Huhtinen, J. Herzog-Arbeitman, A. Chew, B. A. Bernevig, and P. Törmä, Revisiting flat band superconductivity: Dependence on minimal quantum metric and band touchings, Phys. Rev. B **106**, 014518 (2022).

[11] M. Iskin, Effective-mass tensor of the two-body bound states and the quantum-metric tensor of the underlying Bloch states in multiband lattices, Phys. Rev. A **105**, 023312 (2022).

[12] J. Herzog-Arbeitman, V. Peri, F. Schindler, S. D. Huber, and B. A. Bernevig, Superfluid weight bounds from symmetry and quantum geometry in flat bands, Phys. Rev. Lett. **128**, 087002 (2022).

[13] J. Herzog-Arbeitman, A. Chew, K.-E. Huhtinen, P. Törmä, and B. A. Bernevig, Many-body superconductivity in topological flat bands, arXiv:2209.00007 (2022)

[14] F. Piéchon, A. Raoux, J.-N. Fuchs, and G. Montambaux, Geometric orbital susceptibility: Quantum metric without berry curvature, Phys. Rev. B **94**, 134423 (2016).

[15] Y. Gao, S. A. Yang, and Q. Niu, Geometrical effects in orbital magnetic susceptibility, Phys. Rev. B **91**, 214405 (2015).

[16] T. Holder, D. Kaplan, and B. Yan, Consequences of time-reversal-symmetry breaking in the light-matter interaction: Berry curvature, quantum metric, and diabatic motion, Phys. Rev. Res. **2**, 033100 (2020).

[17] G. E. Topp, C. J. Eckhardt, D. M. Kennes, M. A. Sentef, and P. Törmä, Light-matter coupling and quantum geometry in moiré materials, Phys. Rev. B **104**, 064306 (2021).

[18] D. J. Thouless, M. Kohmoto, M. P. Nightingale, and M. den Nijs, Quantized Hall conductance in a two-dimensional periodic potential, Phys. Rev. Lett. **49**, 405 (1982).

[19] Q. Niu, D. J. Thouless, and Y.-S. Wu, Quantized Hall conductance as a topological invariant, Phys. Rev. B **31**, 3372 (1985).

[20] M. Kohmoto, Topological invariant and the quantization of the Hall conductance, Ann. Phys. (NY) **160**, 343 (1985).

[21] M. Onoda and N. Nagaosa, Topological nature of anomalous Hall effect in ferromagnets, J. Phys. Soc. Jpn. **71**, 19 (2002).

[22] T. Jungwirth, Q. Niu, and A. H. MacDonald, Anomalous Hall effect in ferromagnetic semiconductors, Phys. Rev. Lett. **88**, 207208 (2002).

[23] A. Zhang and J.-W. Rhim, Geometric origin of intrinsic spin Hall effect in an inhomogeneous electric field, Commun. Phys. **5**, 195 (2022).

[24] J.-X. Yu, J. Zang, R. K. Lake, Y. Zhang, and G. Yin, Discrete quantum geometry and intrinsic spin Hall effect, Phys. Rev. B **104**, 184408 (2021).

[25] I. Komissarov, T. Holder, and R. Queiroz, The quantum geometric origin of capacitance in insulators, arXiv:2306.08035 (2023).

[26] J.-W. Rhim, K. Kim, and B.-J. Yang, Quantum distance and anomalous landau levels of flat bands, Nature (London) **584**, 59 (2020).

[27] A. Abouelkomsan, K. Yang, and E. J. Bergholtz, Quantum metric induced phases in moiré materials, Phys. Rev. Res. **5**, L012015 (2023).

[28] Y. Gao and D. Xiao, Nonreciprocal directional dichroism induced by the quantum metric dipole, Phys. Rev. Lett. **122**, 227402 (2019).

[29] J. Ahn, G.-Y. Guo, N. Nagaosa, and A. Vishwanath, Riemannian geometry of resonant optical responses, Nat. Phys. **18**, 290 (2021).

[30] M. Iskin, Geometric contribution to the goldstone mode in spin-orbit coupled fermi superfluids, Phys. B: Condens. Mater. **592**, 412260 (2020).

[31] A. Julku, G. M. Bruun, and P. Törmä, Quantum geometry and flat band Bose-Einstein condensation, Phys. Rev. Lett. **127**, 170404 (2021).

[32] A. Gianfrate, O. Bleu, L. Dominici, V. Ardizzone, M. De Giorgi, D. Ballarini, G. Lerario, K. West, L. N. Pfeiffer, D. D. Solnyshkov, D. Sanvitto, and G. Malpuech, Measurement of the quantum geometric tensor and of the anomalous Hall drift, Nature (London) **578**, 381 (2020).

[33] J. P. Provost and G. Vallee, Riemannian structure on manifolds of quantum states, Commun. Math. Phys. **76**, 289 (1980).

[34] Y. Cao, V. Fatemi, S. Fang, K. Watanabe, T. Taniguchi, E. Kaxiras, and P. Jarillo-Herrero, Unconventional superconductivity in magic-angle graphene superlattices, Nature (London) **556**, 43 (2018).

[35] Y. Cao, V. Fatemi, A. Demir, S. Fang, S. L. Tomarken, J. Y. Luo, J. D. Sanchez-Yamagishi, K. Watanabe, T. Taniguchi, E. Kaxiras, R. C. Ashoori, and P. Jarillo-Herrero, Correlated insulator behaviour at half-filling in magic-angle graphene superlattices, Nature (London) **556**, 80 (2018).

[36] M. Yankowitz, S. Chen, H. Polshyn, Y. Zhang, K. Watanabe, T. Taniguchi, D. Graf, A. F. Young, and C. R. Dean, Tuning superconductivity in twisted bilayer graphene, Science **363**, 1059 (2019).

[37] J. M. Park, Y. Cao, K. Watanabe, T. Taniguchi, and P. Jarillo-Herrero, Tunable strongly coupled superconductivity in magic-angle twisted trilayer graphene, Nature (London) **590**, 249 (2021).

[38] C. Shen, Y. Chu, Q. Wu, N. Li, S. Wang, Y. Zhao, J. Tang, J. Liu, J. Tian, K. Watanabe, T. Taniguchi, R. Yang, Z. Meng, D. Shi, O. V. Yazyev, and G. Zhang, Correlated states in twisted double bilayer graphene, Nat. Phys. **16**, 520 (2020).

[39] Y. Cao, D. Rodan-Legrain, O. Rubies-Bigorda, J. M. Park, K. Watanabe, T. Taniguchi, and P. Jarillo-Herrero, Tunable correlated states and spin-polarized phases in twisted bilayer-bilayer graphene, Nature (London) **583**, 215 (2020).

[40] X. Lu, P. Stepanov, W. Yang, M. Xie, M. A. Aamir, I. Das, C. Urgell, K. Watanabe, T. Taniguchi, G. Zhang, A. Bachtold, A. H. MacDonald, and D. K. Efetov, Superconductors, orbital magnets and correlated states in magic-angle bilayer graphene, Nature (London) **574**, 653 (2019).

[41] H. Tian, X. Gao, Y. Zhang, S. Che, T. Xu, P. Cheung, K. Watanabe, T. Taniguchi, M. Randeria, F. Zhang, C. N. Lau, and Marc W. Bockrath, Evidence for flat band Dirac superconductor originating from quantum geometry, Nature **614**, 440 (2023).

[42] L. Balents, C. R. Dean, D. K. Efetov, and A. F. Young, Superconductivity and strong correlations in moiré flat bands, Nat. Phys. **16**, 725 (2020).

[43] E. Y. Andrei, D. K. Efetov, P. Jarillo-Herrero, A. H. MacDonald, K. F. Mak, T. Senthil, E. Tutuc, A. Yazdani, and A. F. Young, The marvels of moiré materials, Nat. Rev. Mater. **6**, 201 (2021).

[44] P. Törmä, S. Peotta, and B. A. Bernevig, Superconductivity, superfluidity and quantum geometry in twisted multilayer systems, Nat. Rev. Phys. **4**, 528 (2022).

[45] D. Leykam, A. Andreanov, and S. Flach, Artificial flat band systems: From lattice models to experiments, Adv. Phys.: X **3**, 1473052 (2018).

[46] J.-W. Rhim and B.-J. Yang, Singular flat bands, Adv. Phys.: X **6**, 1901606 (2021).

[47] G. Bouzerar and D. Mayou, Quantum transport in self-similar graphene carpets, Phys. Rev. Res. **2**, 033063 (2020).

[48] G. Bouzerar and D. Mayou, Quantum transport in flat bands and supermetallicity, Phys. Rev. B **103**, 075415 (2021).

[49] A. Ferreira and E. R. Mucciolo, Critical delocalization of chiral zero energy modes in graphene, Phys. Rev. Lett. **115**, 106601 (2015).

[50] Z. Fan, A. Uppstu, and A. Harju, Anderson localization in two-dimensional graphene with short-range disorder: One-parameter scaling and finite-size effects, Phys. Rev. B **89**, 245422 (2014).

[51] A. Cresti, F. Ortmann, T. Louvet, D. Van Tuan, and S. Roche, Broken symmetries, zero-energy modes, and quantum transport in disordered graphene: From supermetallic to insulating regimes, Phys. Rev. Lett. **110**, 196601 (2013).

[52] M. Vigh, L. Oroszlány, S. Vajna, P. San-Jose, G. Dávid, J. Cserti, and B. Dóra, Diverging dc conductivity due to a flat band in a disordered system of pseudospin-1 Dirac-Weyl fermions, Phys. Rev. B **88**, 161413(R) (2013).

[53] J. Wang, J. F. Liu, and C. S. Ting, Recovered minimal conductivity in the α-T_3 model, Phys. Rev. B **101**, 205420 (2020).

[54] J. Mitscherling and T. Holder, Bound on resistivity in flat-band materials due to the quantum metric, Phys. Rev. B **105**, 085154 (2022).

[55] B. Mera and J. Mitscherling, Nontrivial quantum geometry of degenerate flat bands, Phys. Rev. B **106**, 165133 (2022).

[56] G. Bouzerar, Giant boost of the quantum metric in disordered one-dimensional flat-band systems, Phys. Rev. B **106**, 125125 (2022).

[57] K. Ziegler, Minimal conductivity of graphene: Nonuniversal values from the Kubo formula, Phys. Rev. B **75**, 233407 (2007).

[58] L. Calderín, V. V. Karasiev, and S. B. Trickey, Kubo-Greenwood electrical conductivity formulation and implementation for projector augmented wave datasets, Comput. Phys. Commun. **221**, 118 (2017).

[59] D. A. Greenwood, The Boltzmann equation in the theory of electrical conduction in metals, Proc. Phys. Soc. **71**, 585 (1958).

[60] R. Kubo, Statistical-mechanical theory of irreversible processes. I. General theory and simple applications to magnetic and conduction problems, J. Phys. Soc. Jpn. **12**, 570 (1957).

[61] A. Bastin, C. Lewiner, O. Betbedermatibet, and P. Nozieres, Quantum oscillations of the Hall effect of a fermion gas with random impurity scattering, J. Phys. Chem. Solids **32**, 1811 (1971).

[62] P. Streda, Theory of quantised Hall conductivity in two dimensions, J. Phys. C **15**, L717 (1982).

[63] A. Crépieux and P. Bruno, Theory of the anomalous Hall effect from the Kubo formula and the Dirac equation, Phys. Rev. B **64**, 014416 (2001).

[64] V. Bonbien and A. Manchon, Symmetrized decomposition of the Kubo-Bastin formula, Phys. Rev. B **102**, 085113 (2020).

[65] J. Mitscherling, Longitudinal and anomalous Hall conductivity of a general two-band model, Phys. Rev. B **102**, 165151 (2020).

[66] R. Resta, The insulating state of matter: A geometrical theory, Eur. Phys. J. B **79**, 121 (2011).

[67] D. Xiao, M.-C. Chang, and Q. Niu, Berry phase effects on electronic properties, Rev. Mod. Phys. **82**, 1959 (2010).

[68] S. H. Simon and M. S. Rudner, Contrasting lattice geometry dependent versus independent quantities: Ramifications for Berry curvature, energy gaps, and dynamics, Phys. Rev. B **102**, 165148 (2020).

[69] A. Kruchkov, Quantum transport in dispersionless electronic bands, Phys. Rev. B **107**, L241102 (2023).

[70] J. M. Tomczak and S. Biermann, Optical properties of correlated materials: Generalized Peierls approach and its application to VO_2, Phys. Rev. B **80**, 085117 (2009).

[71] R. Nourafkan and A.-M. S. Tremblay, Hall and Faraday effects in interacting multiband systems with arbitrary band topology and spin-orbit coupling, Phys. Rev. B **98**, 165130 (2018).